Organic Electronics 73 (2019) 13–17

Contents lists available at ScienceDirect

Organic Electronics

journal homepage: www.elsevier.com/locate/orgel

Transparent conductive hybrid thin-films based on copper-mesh/conductive polymer for ITO-Free organic light-emitting diodes

Joo Won Han[a,1], Bogwang Jung[b,1], Dong Woo Kim[a], Kwon Taek Lim[a,*], Se-Young Jeong[b,c,**], Yong Hyun Kim[a,***]

[a] Department of Display Engineering, Pukyong National University, Busan, 48513, Republic of Korea
[b] Department of Cogno-mechatronics Engineering, Pusan National University, Busan, 46241, Republic of Korea
[c] Department of Optics and Mechatronics Engineering, Pusan National University, Busan, 46241, Republic of Korea

ARTICLE INFO

Keywords:
Copper mesh
PEDOT:PSS
Transparent electrodes
Organic light-emitting diodes
Organic electronics

ABSTRACT

We report on highly transparent conductive hybrid thin-films based on copper (Cu)-mesh structures combined with conductive polymer films. The hybrid films show outstanding optical and electrical properties (transmittance of 81.7% at a wavelength of 550 nm, sheet resistance of 71.3 Ω/sq). The effective current collecting property of metal mesh structures as well as the excellent current spreading property of the conducting polymer enables the high performance of the hybrid transparent electrodes. Organic light-emitting diodes (OLEDs) employing the hybrid transparent electrodes result in 2.0-fold enhanced current and power efficiencies, compared to the control polymer electrode-based OLED without current collecting metal mesh structures. The results present that Cu-mesh structures combined with conductive polymer films show great promise for applications in low-cost, flexible indium tin oxide-free OLEDs.

1. Introduction

Organic light-emitting diodes (OLEDs) are attracting much attention as energy-efficient, low-cost, flexible displays and light sources. They have successfully found practical applications in commercial mobile displays and flat panel TVs [1,2]. For next applications in flexible displays and signage, the development of efficient, low-cost transparent conductive electrodes is of great necessity. However, indium tin oxide (ITO), which is the most commonly used transparent electrode, significantly hinders the applications in flexible devices due to its inherent brittleness, elevated processing temperature, and high material cost [3]. In this manner, increasing efforts have been made to develop alternative transparent conductors including graphene [4,5], carbon nanotubes [6,7], metal nanowires [8,9], conductive polymers [10,11], and metal mesh [12–16] to replace the conventional ITO transparent electrode. However, carbon-based electrodes including the conductive polymer, graphene, and carbon nanotube electrodes do not provide sufficient electrical properties especially for large-area devices. In addition, metal nanowires as well as carbon nanotubes cause a significant electrical leakage of organic devices due to the inherent roughness of electrodes [7,17,18].

The low conductivity of poly(3,4-ethylenedioxythiophene):poly (styrenesulfonate) (PEDOT:PSS) films can be compensated by the introduction of the metal mesh or grid structures, which provide excellent electrical and thermal properties. Scaling-up ITO-free organic devices to larger areas indeed requires such metal structures for efficient and homogeneous charge collection/distribtuion. We firstly reported silver (Ag) grid/fullerene C_{60} hybrid transparent electrodes which were successfully integrated in ITO-free organic photovoltaic (OPV) cells [19]. The transparent electrodes based on the silver (Ag) grid/ultra-transparent PEDOT:PSS films in our previous study also show the outstanding electrode performance (an average transmittance of 90% at a visible wavelength with a sheet resistance of 8.7 Ω/sq) and the power conversion efficiency (PCE) of ITO-free OPV cell with the hybrid electrode was comparable to that of the ITO-reference OPV cells [14]. In addition, we have succeeded to grow single-crystal copper (Cu) films on sapphire substrate in high quality [20]. Based on the films, we fabricated ZnO/Cu honeycomb mesh on polyimide substrates, showing outstanding conductivity, transmittance and mechanical flexibility [21]. The fabricated films with mesh structures (a 30 μm hexagonal

* Corresponding author.
** Corresponding author. Department of Cogno-mechatronics Engineering, Pusan National University, Busan, 46241, Republic of Korea.
*** Corresponding author.
E-mail addresses: ktlim@pknu.ac.kr (K.T. Lim), syjeong@pusan.ac.kr (S.-Y. Jeong), yhkim113@pknu.ac.kr (Y.H. Kim).
[1] These authors contributed equally to this work.

https://doi.org/10.1016/j.orgel.2019.05.018
Received 7 March 2019; Received in revised form 27 April 2019; Accepted 11 May 2019
Available online 31 May 2019
1566-1199/

open area size and a 2 μm line-width) exhibited a sheet resistance of 6.2 Ω/sq with a high transmittance of 90.7%. The Cu mesh (Cu-M) electrodes showed high mechanical and electrical stabilities after 1,000 cycles of bending stress test. While most works for metal mesh as well as metal nanowires have been devoted to Ag-based material, few studies of OLEDs integrated with Cu-M or Cu nanowires have been reported so far [22–24]. Cu-based transparent electrodes have attracted interest recently, which can substantially reduce the material cost while obtaining enough conductivity for the use in transparent electrodes, that seems promising for low-cost organic devices [17,18]. Moreover, metal mesh structures patterned by a conventional UV lithographic method give reliable, straightforward properties, compared to screen- or inkjet-printed meshes due to industry proven reliability [25,26].

Here, we demonstrate highly transparent conductive hybrid thin-films composed of Cu-M/ PEDOT:PSS as a transparent electrode for ITO-free OLEDs. The current collecting Cu-M structures are prepared using a reliable lithographic method, showing the uniformly formed structures and the significantly reduced resistance of the PEDOT:PSS films. The conductive PEDOT:PSS on the Cu-M structures flattens the metal mesh structures to prevent the electrical leakages of OLEDs and provides the uniform spread of electrical currents over the electrode films. The optimized hybrid transparent electrode exhibits an optical transmittance of 81.7% at a wavelength of 550 nm with a low sheet resistance of 71.3 Ω/sq. Furthermore, the OLEDs fabricated with the Cu-M/PEDOT:PSS transparent electrodes show greatly improved current and power efficiencies (by a factor of 2.0 compared to that of the PEDOT:PSS-based OLED), the reduced operating voltages, and the enhanced luminance of devices. The Cu-M/PEDOT:PSS shows great promise for the replacement of ITO in low-cost and flexible ITO-free OLEDs.

2. Experimental

2.1. Preparation of Cu-M films

The high-quality single crystal Cu thin-film was prepared by the support of Crystal Bank (NRF-2013M3A9B8030390) in Pusan National University. The wafer-scale single-crystal Cu thin-film was prepared on a single crystal sapphire (0001) plane by a radio frequency (RF) sputtering process. The applied RF power was 40 W and the deposition rate and the basal pressure were of 0.1 nm s^{-1} and 10^{-3} Torr, respectively. The optimum condition of the substrate temperature was 195 ± 2 °C. The high-quality single-crystal Cu (111) target was used in the sputtering process and additional conditions such as RF power, substrate temperature, and vacuum atmosphere were optimized to obtain a high quality single-crystal Cu (111) film on sapphire substrates [20].

For the fabrication of a honeycomb mesh structure using the single-crystal Cu thin-film, a photoresist layer (AZ5214, AZ Electronic Materials) was spin-coated on the Cu thin-films at 4000 rpm and the honeycomb mesh structure was defined onto the photoresist layer via UV lithography. The UV light -exposed area on the photoresist layer was removed by a developer (MIF300, AZ Electronic Materials) and the patterned film was hard-baked. The samples were wet-etched with a Cu etchant at 25 °C [21]. We fixed the hexagonal open area size and the line-width in the honeycomb mesh to be 30 μm and 2 μm, respectively. The patterned structures were confirmed through the atomic force microscopy (AFM) and scanning electron microscope (SEM) observations.

2.2. Fabrication and characterization of Cu-M/PEDOT:PSS electrode

PEDOT:PSS (Clevios PH1000, Heraeus) solutions were mixed with 6 vol% of ethylene glycol. The mixed PEDOT:PSS solutions were spin-coated at 1500 rpm for 30 s on bare glass substrates or Cu-M films, which were pre-treated by plasma for 10 min. The films were subsequently annealed on a hot plate at 120 °C for 10 min in ambient atmosphere. The resulting thickness of Cu-M/PEDOT:PSS films is about 100 nm. The sheet resistance of the films was characterized by the van der Pauw method with a sourcemeter (Keithley 2401). The transmittance of films was examined by a UV-vis spectrophotometer (Optizen pop, MECASYS). The surface images of films were obtained using scanning electron microscope (SEM, S-2400 Hitachi) and atomic force microscopy (AFM, Icon-PT-PLUS, BRUKER).

2.3. Fabrication and characterization of OLEDs

The solution-processed OLEDs were fabricated in the ambient air. The 35 nm-thick PEDOT:PSS (AI4083, Heraeus) hole transport layer was spin-coated at 1500 rpm for 30 s onto the PEDOT:PSS or Cu-M/PEDOT:PSS electrodes. The emissive layer (EML) was prepared with a blend of poly(9-vinylcarbazole) (PVK), 4,4′-N,N′-dicarbazole-biphenyl (CBP) as cohosts, and tris[2-(p-tolyl)pyridine]iridium(III) ($Ir(mppy)_3$ as the green phosphorescent dopant dissolved in chlorobenzene at a concentration of 10 mg/mL with a blend ratio of 0.45:0.45:0.1 by weight. The EML was spin-coated at a spin speed of 800 rpm, and the film was annealed at 100 °C. The resulting thickness of EML is about 60 nm. Subsequently, 2,2′,2″-(1,3,5-Benzinetriyl)-tris(1-phenyl-1-H-benzimidazole) (TPBi) as an electron transport layer (ETL) dissolved in methanol was spin-coated on the EML, resulting in the thickness of 20 nm. LiF (1 nm) and Al (70 nm) were deposited on the ETL via thermal evaporation. The device showed an active area of about 6 mm^2. The OLED performances were recorded by a spectroradiometer (CS-2000, Minolta) and source-measure unit system (Keithley 2401).

3. Results and Discussion

Fig. 1 shows the crystallographic data of the Cu thin-film used in this study. XRD patterns (Fig. 1a) show only two peaks corresponding to the Al_2O_3 (0001) plane (41.675°) and the Cu (111) plane (43.295°), which means that the sample is aligned well in a single phase along to (111). The root-mean-square (RMS) roughness for the Cu film measured by AFM (Fig. 1b) is 0.394 nm and no distinct grain boundaries are observed from the SEM images of both 1 μm scale and 100 nm scale (Fig. 1c). Electron backscattering diffraction (EBSD) map (Fig. 1d) reveals that the sputtered Cu thin-film is aligned to the (111) orientation and the sole spots associated with the (111) direction are distinct in inverse pole figures (IPFs), which reflects that the Cu film is deposited with a single crystal quality. {100} pole figures are visible with six primary spots, while the {100} pole figure should hold an ideal cubic three-fold symmetry, which implies the presence of twin boundaries in the sputtered Cu thin-film. Detailed study about the formation of twin boundaries will be discussed separately.

Fig. 2 exhibits the transmittance spectra for PEDOT:PSS, Cu-M, and Cu-M/PEDOT:PSS transparent electrodes. The sophisticated patterning for the Cu film is performed by lithography method where the diameter and line-width of Cu-M investigated here are 30 μm and 2 μm, respectively. The sheet resistance and transmittance values for the electrodes are summarized in Table 1. The transmittances of PEDOT:PSS, Cu-M, and Cu-M/PEDOT:PSS are 94.6, 85.7, and 81.7%, respectively, at a wavelength of 550 nm. By introducing Cu-M, the sheet resistance of PEDOT:PSS greatly drops from 100.7 to 71.3 Ω/sq, indicating that the effective current pathways are formed through current collecting Cu-M on the resistive PEDOT:PSS films. These results suggest that the PEDOT:PSS electrode needs to be combined with metal grid structures for providing the additional electrical conductivity, especially for large-area cells. The mesh structure formed on the PEDOT:PSS reinforces the electrical property of the PEDOT:PSS film while the transmittance is inevitably reduced. Due to the trade-off between the conductivity and transmittance, the optimization process of Cu-M including the control of thickness and the line-width/pitch and of mesh structures is of importance, which will be studied in our future work.

The SEM images of PEDOT:PSS, Cu-M, and Cu-M/PEDOT:PSS are

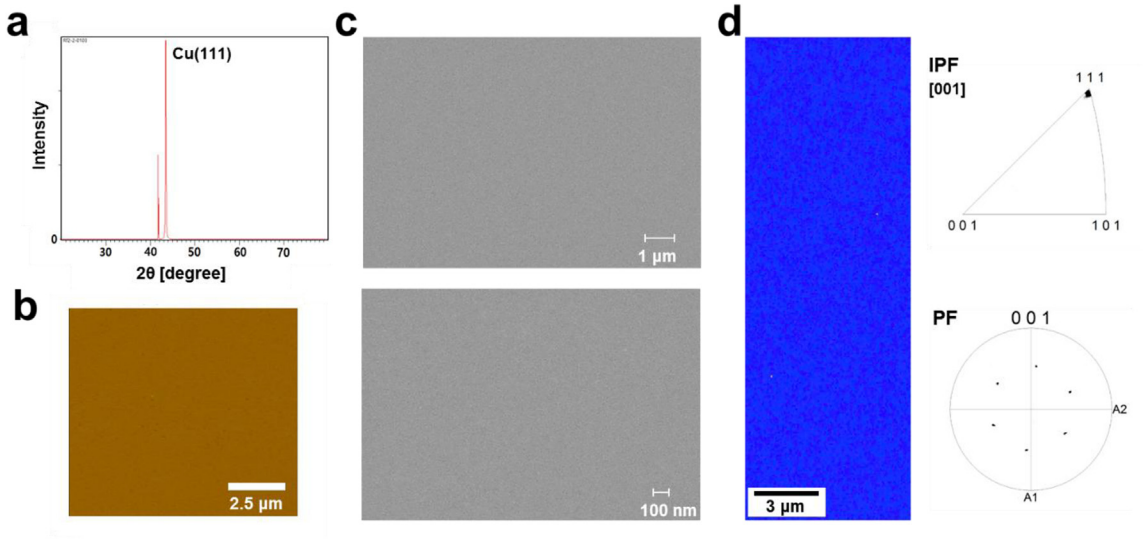

Fig. 1. (a) XRD pattern, (b) AFM, (c) SEM images, and (d) EBSD map for the Cu thin-film.

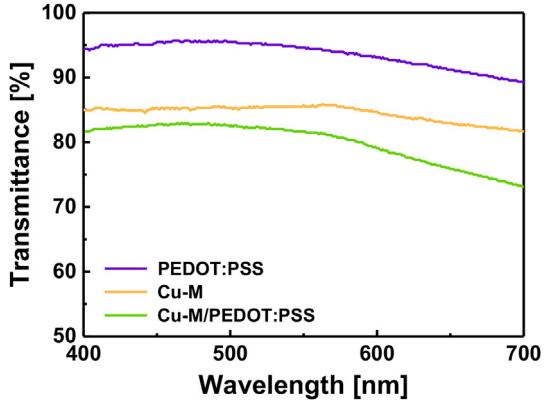

Fig. 2. Transmittance spectra for PEDOT:PSS, Cu-M, and Cu-M/PEDOT:PSS transparent electrodes.

Table 1
Sheet resistance and transmittance for PEDOT:PSS and Cu-M/PEDOT:PSS transparent electrodes.

	Sheet resistance [Ω/sq]	Transmittance @550 nm [%]
PEDOT:PSS	100.7	94.6
Cu-M/PEDOT:PSS	71.3	81.7

shown in Fig. 3. The PEDOT:PSS film without any structure shows a typical flat surface (Fig. 3a). The Cu-M without PEDOT:PSS exhibits well-defined, uniform honeycomb mesh structures with a diameter of 30 μm and a line-width of 2 μm (Fig. 3b). The honeycomb structures used in our work can provide a homogeneous current distribution. The flattened mesh structures are observed for Cu-M/PEDOT:PSS by the overcoated PEDOT:PSS film, which does not reflect the original electrode topography (Fig. 3c).

Fig. 4 demonstrates the AFM images for PEDOT:PSS, Cu-M, and Cu-M/PEDOT:PSS electrodes. Cu-M fabricated on the glass substrate clearly exhibits a honeycomb structure (Fig. 4b and c). The RMS roughness value for PEDOT:PSS without the mesh structure is about 2.0 nm (area of $10 \times 10\,\mu m^2$). Since the soared mesh structure can cause a damage of organic layers with a large leakage current of devices, it is of great necessity to introduce a planar layer to lower the surface roughness in the transparent electrode for preventing the deterioration of device performance. The RMS roughness value of Cu-M with overcoated PEDOT:PSS is about 14.2 nm which is still in an adequate level not to produce a serious leakage current of devices.

To figure out the electrode performance of the Cu-M/PEDOT:PSS-based film, we fabricate solution-processed green OLEDs built on the PEDOT:PSS film and the Cu-M/PEDOT:PSS film as shown in Fig. 5. Fig. 6a and b exhibit the current density-voltage (*J-V*) and the luminance-voltage (*L-V*) characteristics of devices, respectively. The current density of the OLED based on the Cu-M/PEDOT:PSS is much higher than that of the reference OLED with PEDOT:PSS at given voltages, which is attributed to the over-injected charges by highly conductive Cu-M. The OLED based on Cu-M/PEDOT:PSS presents a higher luminance compared to that of the PEDOT:PSS-based OLED owing to the effect of electrical enhancement of the anode. In addition, the Cu-M/PEDOT:PSS-based OLED shows a greatly reduced turn-on voltage of 3.6 V compared to the PEDOT:PSS-based control device (5.6 V) although the work function of Cu-M (~4.7 eV) is lower than that of

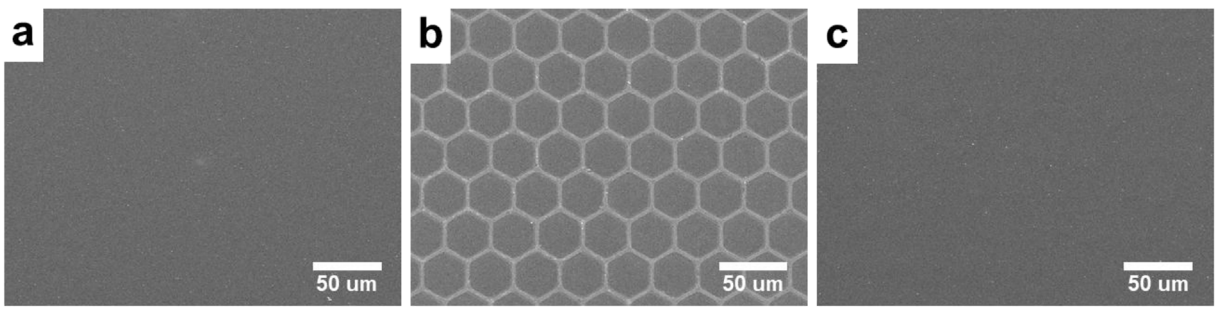

Fig. 3. SEM images of (a) PEDOT:PSS, (b) Cu-M, and (c) Cu-M/PEDOT:PSS transparent electrodes.

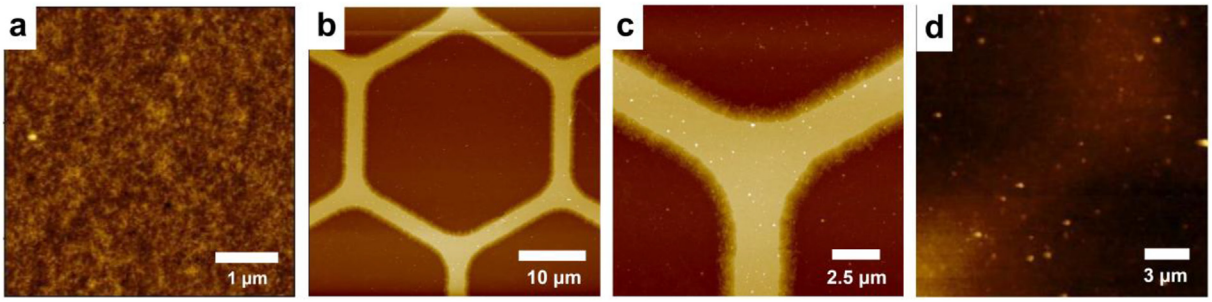

Fig. 4. AFM topography images of (a) PEDOT:PSS, (b, c) Cu-M, and (d) Cu-M/PEDOT:PSS films.

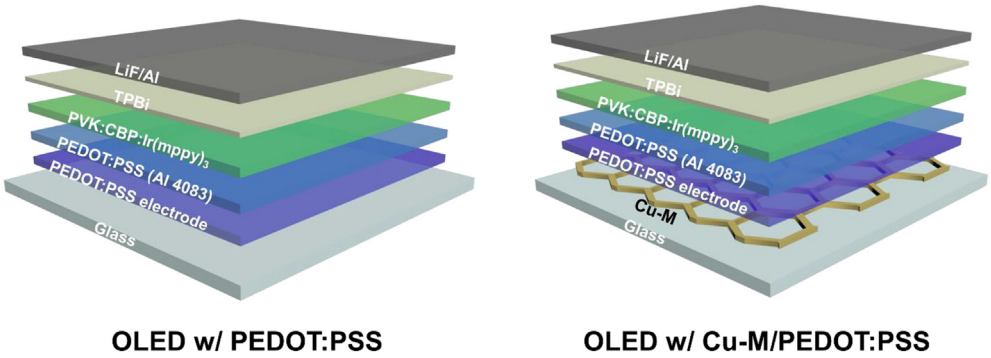

Fig. 5. Schematic illustrations of OLEDs (a) with PEDOT:PSS and (b) with Cu-M/PEDOT:PSS transparent electrodes.

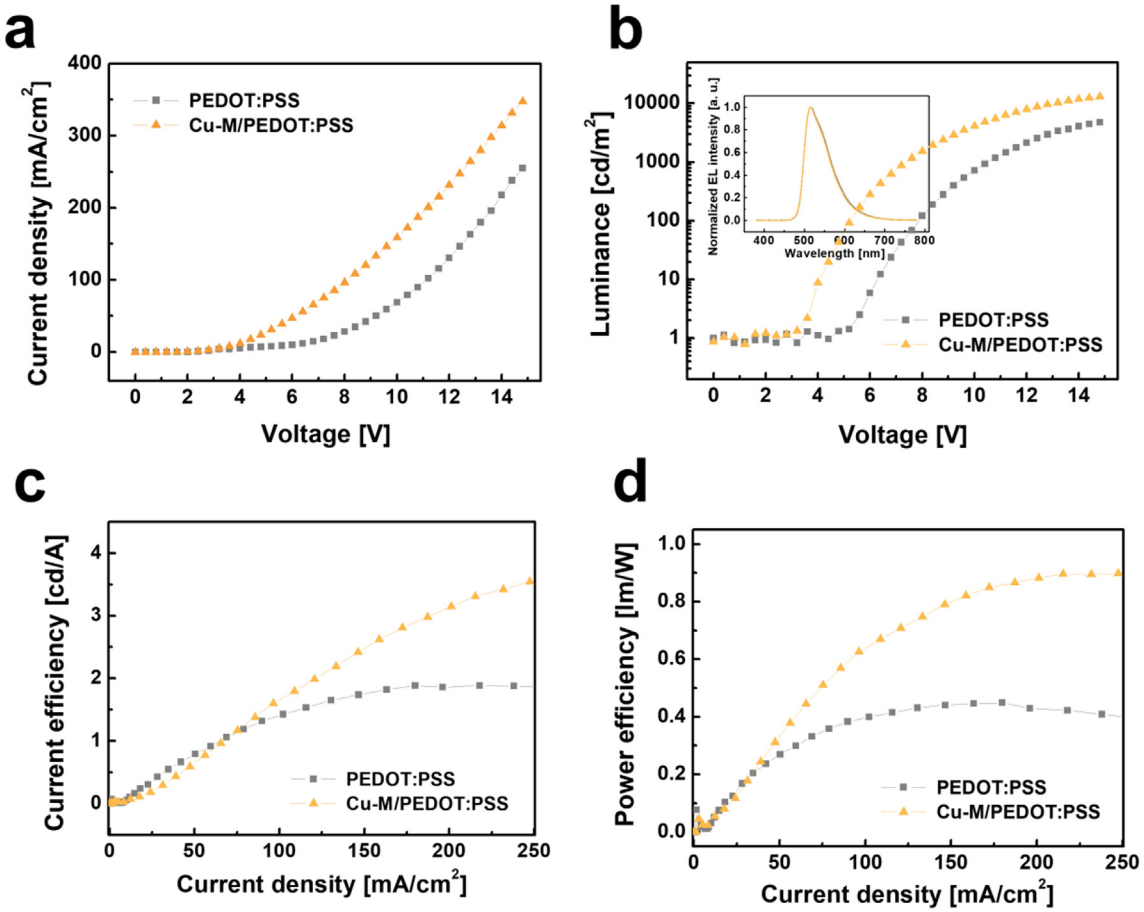

Fig. 6. (a) Current density-voltage, (b) luminance-voltage, (c) current efficiency, and (d) power efficiency characteristics of OLEDs with PEDOT:PSS and Cu-M/PEDOT:PSS transparent electrodes. Inset in (b): Electroluminescence (EL) intensity of OLEDs.

Table 2
The performance of OLEDs with PEDOT:PSS and Cu-M/PEDOT:PSS transparent electrodes.

	current efficiency [max] [cd/A]	power efficiency [max] [lm/W]
OLED w/ PEDOT:PSS	1.9	0.45
OLED w/ Cu-M/PEDOT:PSS	3.8	0.9

PEDOT:PSS (~5.1 eV). The higher luminance and the reduced turn-on voltage of the Cu-M/PEDOT:PSS-based OLED are attributed to the highly reduced resistance of the anode assisted by the highly conductive Cu-M. The well-formed Cu-M structures enhance the injection of charges and the PEDOT:PSS layer effectively flattens the Cu-M, preventing carrier loss from the leakage current and also acts as a current spreading layer. The electroluminescence (EL) spectrum of the Cu-M/PEDOT:PSS-based OLED is almost identical to that of the PEDOT:PSS-based OLED, indicating that the mesh structures in the device barely affect on emission color.

Fig. 6c and d show the current efficiency (CE) and the power efficiency (PE) for the devices, respectively, and the values are summarized in Table 2. The OLED with Cu-M/PEDOT:PSS displays the significantly higher efficiencies than the control device with PEDOT:PSS with the help of the low operating voltage and the outstanding current injection characteristic. The highest CE of the Cu-M/PEDOT:PSS-based OLED reaches over 3.8 cd/A with an improvement by a factor of 2.0 with respect to the reference PEDOT:PSS-based OLED (1.9 cd/A). The maximum PE of the OLED with Cu-M/PEDOT:PSS is improved by a factor of 2.0, corresponding to 0.9 lm/W, compared to that of the OLED with PEDOT:PSS (0.45 lm/W), indicating that the metal mesh structure effectively reduces operating voltages and enhances the luminance of device. The angular emission characteristics and angle-dependent spectra for both devices are almost equal (Figs. S1 and S2 in the Supporting Information). The angle-dependent spectral distortion is not observed for Cu-M/PEDOT:PSS-based OLED despite of the optically reflective metal structures. As the control of the line-width and diameter for mesh structures is of importance to maximize the performance of Cu-M-based OLEDs, the size effect (line-width/pitch and grid height) of mesh structures on the performance of OLEDs will be studied in our future work.

4. Conclusion

We demonstrate the highly conductive Cu-M/PEDOT:PSS transparent conductive thin-films as a transparent electrode for ITO-free OLEDs. The current collecting Cu-M structures effectively decrease the resistance of the PEDOT:PSS films. In addition, the conductive PEDOT:PSS polymer successfully flattens the metal mesh structures and uniformly spreads currents over the films. The hybrid Cu-M/PEDOT:PSS transparent electrodes achieve a high transmittance of 81.7% at a wavelength of 550 nm and a low sheet resistance of 71.3 Ω/sq. The CE and PE of the OLED based on the Cu-M/PEDOT:PSS transparent electrodes are greatly improved by a factor of 2.0 compared to that of the PEDOT:PSS-based OLED, attributed to the combined effects of the reduced operating voltage and the enhanced luminance of the device. Our results demonstrate that Cu-M/PEDOT:PSS can serve as a promising transparent electrode for low-cost and flexible ITO-free OLEDs.

Acknowledgments

This research was supported by Basic Science Research Program through the National Research Foundation of Korea funded by the Ministry of Science, ICT & Future Planning (2016R1C1B2012490) and partly by (2017R1A2B3011822).

Appendix A. Supplementary data

Supplementary data to this article can be found online at https://doi.org/10.1016/j.orgel.2019.05.018.

References

[1] S. Reineke, M. Thomschke, B. Lüssem, K. Leo, White organic light-emitting diodes: status and perspective, Rev. Mod. Phys. 85 (2013) 1245–1293.
[2] S. Reineke, Complementary LED technologies, Nat. Mater. 14 (2015) 459–462.
[3] C.J.M. Emmott, A. Urbina, J. Nelson, Environmental and economic assessment of ITO-free electrodes for organic solar cells, Sol. Energy Mater. Sol. Cells 97 (2012) 14–21.
[4] T. Kobayashi, M. Bando, N. Kimura, K. Shimizu, K. Kadono, N. Umezu, K. Miyahara, S. Hayazaki, S. Nagai, Y. Mizuguchi, Y. Murakami, D. Hobara, Production of a 100-m-long high-quality graphene transparent conductive film by roll-to-roll chemical vapor deposition and transfer process, Appl. Phys. Lett. 102 (2013) 023112.
[5] X. Huang, Z. Zeng, Z. Fan, J. Liu, H. Zhang, Graphene-based electrodes, Adv. Mater. 24 (2012) 5979–6004.
[6] Y.H. Kim, L. Müller-Meskamp, A. a. Zakhidov, C. Sachse, J. Meiss, J. Bikova, A. Cook, A. a. Zakhidov, K. Leo, Semi-transparent small molecule organic solar cells with laminated free-standing carbon nanotube top electrodes, Sol. Energy Mater. Sol. Cells 96 (2012) 244–250.
[7] D.S. Hecht, L. Hu, G. Irvin, Emerging transparent electrodes based on thin films of carbon nanotubes, graphene, and metallic nanostructures, Adv. Mater. 23 (2011) 1482–1513.
[8] Z.R. Ramadhan, J.W. Han, D.J. Lee, S.A.N. Entifar, J. Hong, C. Yun, Y.H. Kim, Surface-functionalized silver nanowires on chitosan biopolymers for highly robust and stretchable transparent conducting films, Mater. Res. Lett. 7 (2019) 124–130.
[9] D.W. Kim, J.W. Han, K.T. Lim, Y.H. Kim, Highly enhanced light-outcoupling efficiency in ITO-free organic light-emitting diodes using surface nanostructure embedded high-refractive index polymers, ACS Appl. Mater. Interfaces 10 (2018) 985–991.
[10] Y.H. Kim, C. Sachse, M.L. Machala, C. May, L. Müller-Meskamp, K. Leo, Highly conductive PEDOT:PSS electrode with optimized solvent and thermal post-treatment for ITO-free organic solar cells, Adv. Funct. Mater. 21 (2011) 1076–1081.
[11] Y.H. Kim, J. Lee, S. Hofmann, M.C. Gather, L. Müller-Meskamp, K. Leo, Achieving high efficiency and improved stability in ITO-free transparent organic light-emitting diodes with conductive polymer electrodes, Adv. Funct. Mater. 23 (2013) 3763–3769.
[12] Y.H. Kim, S. Schubert, R. Timmreck, L. Müller-Meskamp, K. Leo, Collecting the electrons on n-doped fullerene C 60 transparent conductors for all-vacuum-deposited small-molecule organic solar cells, Adv. Energy Mater. 3 (2013) 1551–1556.
[13] Y. Galagan, B. Zimmermann, E.W.C. Coenen, M. Jørgensen, D.M. Tanenbaum, F.C. Krebs, H. Gorter, S. Sabik, L.H. Slooff, S.C. Veenstra, J.M. Kroon, R. Andriessen, Current collecting grids for ITO-free solar cells, Adv. Energy Mater. 2 (2012) 103–110.
[14] Y.H. Kim, L. Müller-Meskamp, K. Leo, Ultratransparent polymer/semitransparent silver grid hybrid electrodes for small-molecule organic solar cells, Adv. Energy Mater. 5 (2015) 1401822.
[15] S. Park, J.T. Lim, W.Y. Jin, H. Lee, B.H. Kwon, N.S. Cho, J.H. Han, J.W. Kang, S. Yoo, J.I. Lee, Efficient large-area transparent OLEDs based on a laminated top electrode with an embedded auxiliary mesh, ACS Photonics 4 (2017) 1114–1122.
[16] C. Peng, C. Chen, K. Guo, Z. Tian, W. Zhu, T. Xu, B. Wei, Organic light-emitting diodes using novel embedded al gird transparent electrodes, Phys. E Low-Dimensional Syst. Nanostructures. 87 (2017) 118–122.
[17] S. Ye, A.R. Rathmell, Z. Chen, I.E. Stewart, B.J. Wiley, Metal nanowire networks: the next generation of transparent conductors, Adv. Mater. 26 (2014) 6670–6687.
[18] T. Sannicolo, M. Lagrange, A. Cabos, C. Celle, J.P. Simonato, D. Bellet, Metallic nanowire-based transparent electrodes for next generation flexible devices: a review, Small 12 (2016) 6052–6075.
[19] Y.H. Kim, S. Schubert, R. Timmreck, L. Müller-Meskamp, K. Leo, Collecting the electrons on n-doped fullerene C 60 transparent conductors for all-vacuum-deposited small-molecule organic solar cells, Adv. Energy Mater. 3 (2013) 1551–1556.
[20] S. Lee, J.Y. Kim, T.-W. Lee, W.-K. Kim, B.-S. Kim, J.H. Park, J.-S. Bae, Y.C. Cho, J. Kim, M.-W. Oh, C.S. Hwang, S.-Y. Jeong, Fabrication of high-quality single-crystal Cu thin films using radio-frequency sputtering, Sci. Rep. 4 (2015) 6230.
[21] W.K. Kim, S. Lee, D. Hee Lee, I. Hee Park, J. Seong Bae, T. Woo Lee, J.Y. Kim, J. Hun Park, Y. Chan Cho, C. Ryong Cho, S.Y. Jeong, Cu mesh for flexible transparent conductive electrodes, Sci. Rep. 5 (2015) 1–8.
[22] C. Sachse, N. Weiß, N. Gaponik, L. Müller-Meskamp, A. Eychmüller, K. Leo, ITO-Free, Small-Molecule organic solar cells on spray-coated copper-nanowire-based transparent electrodes, Adv. Energy Mater. 4 (2014) 1300737.
[23] H.-G. Im, S.-H. Jung, J. Jin, D. Lee, J. Lee, D. Lee, J.-Y. Lee, I.-D. Kim, B.-S. Bae, Flexible transparent conducting hybrid film using a surface-embedded copper nanowire network: a highly oxidation-resistant copper nanowire electrode for flexible optoelectronics, ACS Nano 8 (2014) 10973–10979.
[24] W. Zhou, J. Chen, Y. Li, D. Wang, J. Chen, X. Feng, Z. Huang, R. Liu, X. Lin, H. Zhang, B. Mi, Y. Ma, Copper mesh templated by breath-figure polymer films as flexible transparent electrodes for organic photovoltaic devices, ACS Appl. Mater. Interfaces 8 (2016) 11122–11127.
[25] H.I. Smith, A review of submicron lithography, Superlattice. Microst. 2 (1986) 129–142.
[26] D. McCoul, W. Hu, M. Gao, V. Mehta, Q. Pei, Recent advances in stretchable and transparent electronic materials, Adv. Electron. Mater. 2 (2016) 1500407.